ACS APPLIED MATERIALS & INTERFACES

Research Article

www.acsami.org

Hybrid Lithium–Sulfur Batteries with a Solid Electrolyte Membrane and Lithium Polysulfide Catholyte

Xingwen Yu,[†] Zhonghe Bi,[‡] Feng Zhao,*[,‡] and Arumugam Manthiram*[,†]

[†]Electrochemical Energy Laboratory, Materials Science and Engineering Program, The University of Texas at Austin, Austin, Texas 78712, United States

[‡]Ceramatec, Inc., Salt Lake City, Utah 84119, United States

Supporting Information

ABSTRACT: Lithium–sulfur (Li–S) batteries are receiving great attention as the most promising next-generation power source with significantly high charge-storage capacity. However, the implementation of Li–S batteries is hampered by a critical challenge because of the soluble nature of the intermediate polysulfide species in the liquid electrolyte. The use of traditional porous separators unavoidably allows the migration of the dissolved polysulfide species from the cathode to the lithium–metal anode and results in continuous loss of capacity. In this study, a LiSICON (lithium super ionic conductor) solid membrane is used as a cation-selective electrolyte for lithium–polysulfide (Li-PS) batteries to suppress the polysulfide diffusion. Ionic conductivity issue at the lithium metal/solid electrolyte interface is successfully addressed by insertion of a "soft", liquid–electrolyte integrated polypropylene interlayer. The solid LiSICON lithium-ion conductor maintains stable ionic conductivity during the electrochemical cycling of the cells. The Li-PS battery system with a hybrid solid/liquid electrolyte exhibits significantly enhanced cyclability relative to the cells with the traditional liquid–electrolyte integrated porous separator.

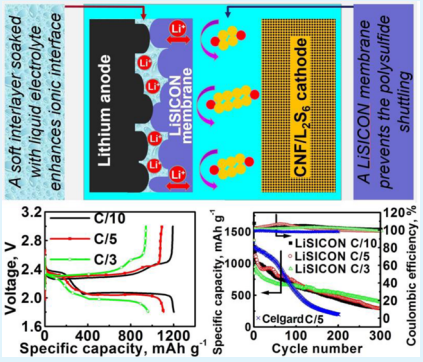

KEYWORDS: *lithium–sulfur batteries, solid electrolyte, polysulfide catholyte, ionic interface, electrochemistry*

1. INTRODUCTION

Depletion of fossil fuels and the increased concern on environmental pollution issues have inspired the society to develop reliable strategies of using renewable energy sources. However, the desired energy sources, for example, solar and wind, are intermittent and need efficient storage and utilization. Furthermore, as one of the major sectors of energy consumption and air pollution, the transportation needs electrification. Electrochemical energy storage in the form of rechargeable batteries is one of the most promising strategies for these applications.[1−4] Among the various rechargeable battery chemistries, lithium-ion batteries, which have the highest energy densities (100–200 Wh/kg), are appealing for both vehicle and grid storage applications.[5] However, for the large scale applications, high-energy density and low-cost battery systems are needed.

With an aim to increase the energy density, lithium–sulfur (Li–S) battery is one of the most promising systems.[6,7] The earth-abundant element sulfur can reversibly undergo a two-electron reaction per sulfur atom with lithium to give Li_2S, leading to a high theoretical capacity of 1675 mAh g^{-1}, which is an order of magnitude higher than those of the currently used transition-metal oxide cathodes.[6,7] However, through many years of efforts, Li–S batteries are still hampered by short cycle life with low electrochemical utilization of the active material.[8] Sulfur occurs as an eight-atom (S_8) ring structure with an orthorhombic symmetry at room temperature. During the discharge reaction with a lithium metal anode, sulfur first forms a series of lithium polysulfides, for example, Li_2S_8, Li_2S_6, and Li_2S_4, and then the final discharge products Li_2S_2 or Li_2S. The polysulfide intermediates produced are soluble in the organic electrolytes that are commonly used in the Li–S batteries.[9] Traditional separators, such as the Celgard-series of materials, have commonly been used for Li–S battery development. However, the use of such porous separators unavoidably allows the migration of the dissolved polysulfide species from the cathode to the lithium–metal anode and induces the shuttling behavior, which consequently results in the loss of active material and capacity degradation.[10] During the past few years, many attempts have been made to encapsulate polysulfides in the cathode through the development of advanced cathode structures.[11−15] However, these conventional approaches are not able to effectively prevent the polysulfide migration through the porous separators. Nonporous, highly Li-ion conductive separator materials are urgently needed to address the polysulfide migration issues.

Use of solid Li-ion conductive electrolyte provides the possibility of avoiding the polysulfide migration problem. However, although previous work on all solid-state Li–S batteries show high Coulombic efficiency, the utilization of

Received: May 14, 2015
Accepted: July 10, 2015
Published: July 10, 2015

DOI: 10.1021/acsami.5b04209
ACS Appl. Mater. Interfaces 2015, 7, 16625–16631

active material and cycle life are not high enough for practical applications.[16−20] In addition, elevated temperature is needed for some of these batteries due to the low ionic conductivity ($<1 \times 10^{-4}$ S cm^{-1}) of the solid-state electrolyte at room temperature. Therefore, use of liquid electrolyte is still necessary toward sufficiently utilizing the sulfur cathode at the low temperatures. Actually, in a Li−S battery system, the dissolution nature of the polysulfides in the electrolyte has dual-effects. In addition to the negative effect of polysulfide shuttling, the dissolution of polysulfides play a positive role for efficient use of the nonconductive sulfur cathode.[21] In the sulfur−carbon composite electrodes, without the dissolution of polysulfides, the reduction of the nonconductive sulfur can only occur on the sulfur−carbon interface and the bulk sulfur cannot be utilized, resulting in low specific capacity. By taking advantage of the soluble polysulfides, recently a particularly interesting approach that uses liquid-phase lithium polysulfide (so-called catholyte) dispersed onto free-standing conductive matrix as the active cathode material has become attractive.[21−23] This novel approach shows facile dispersion and homogeneous distribution of the sulfur active material onto the conductive matrix, and the demonstrated Li/dissolved polysulfide (Li-PS) batteries show a higher utilization of the sulfur active material.[22,23] However, such a Li-PS battery system still suffers from the polysulfide shuttling behavior when the porous Celgard membrane is used.

To eliminate the shuttle effect of polysulfide, we present herein a hybrid Li-PS battery system by employing a solid lithium super ionic conductor (LiSICON) membrane. Use of solid electrolyte for Li-ion batteries have previously been investigated.[24,25] More recently, a novel Li−S battery system was developed with a dual-phase electrolyte, in which a ceramic lithium superionic conductor (LiSICON) film was used to separate the liquid electrolytes for the cathode and the anode.[26] On the basis of a novel cell configuration design, the feasibility of using a solid Li-ion conductor in the Li−S battery system has been proved.[26] In light of the above studies regarding the utilization of the solid electrolytes, properties of the LiSICON membrane, and the characteristics of the Li−S battery system, the key foci of the present study include the following: (1) retention of polysulfides by the LiSICON membrane, (2) cyclability enhancement of the hybrid Li-PS batteries with the LiSICON solid electrolyte, (3) enhancement of the ionic interface between the Li-metal anode and the solid LiSICON membrane,(4) ionic conductivity maintenance of the LiSICON membrane during the cycling of the hybrid Li-PS batteries, and (5) high capacity hybrid Li-PS batteries.

2. MATERIALS AND METHODS

2.1. Chemicals and Materials. The chemicals used for preparation of liquid electrolyte and polysulfide catholytes include the followings: dimethoxy ethane (DME, 99+ %, Acros Organics), 1,3-dioxolane (DOL, 99.5%, Acros Organics), lithium trifluoromethanesulfonate ($LiCF_3SO_3$, 98%, Acros Organics), lithium nitrate ($LiNO_3$, 99+ %, Acros Organics), sublimed sulfur powder (99.5%, Acros Organics), and lithium sulfide (Li_2S, 99.9%, Acros Organics). The carbon nanofiber (CNF, 50−200 μm long, ∼100 nm diameter) powder was purchased from Pyrograf Products Inc. (PR-24-XT-PS). The activated carbon powder (Dacro KB, ∼1500 m^2 g^{-1} surface area) was purchased from Sigma-Aldrich. The LiSICON solid−electrolyte membranes with a composition of $Li_{1.3}Al_{0.3}Ti_{1.7}(PO_4)_3$ were provided by Ceramatec, Inc. The membranes are in the form of circular discs with 16 mm diameter and ∼300 or ∼350 μm thick.

2.2. Synthesis of Polysulfide Catholyte. Blank electrolyte was prepared by dissolving appropriate amounts of $LiCF_3SO_3$ and $LiNO_3$ in a mixed DME and DOL solvent to render a 1.0 M $LiCF_3SO_3$ and 0.1 M $LiNO_3$ solutions. To prepare the dissolved polysulfide catholyte, sublimed sulfur powder and an appropriate amount of Li_2S were added to a proper amount of blank electrolyte to render 1.5 and 4.0 M sulfur in the form of Li_2S_6 in the solution. The solution mixture was heated at 45 °C in an Ar-filled glovebox for 18 h to produce a dark yellow solution with moderate viscosity.

2.3. Synthesis of Free-Standing, Binder-Free Carbon Nanofiber (CNF) Fabric Electrodes and Carbon Nanofiber/Activated Carbon (CNF/AC) Composite Electrodes. To fabricate the self-weaving, free-standing CNF fabric electrodes, 48.0 mg of CNF powder was dispersed in 500 mL of deionized (DI) water by high-power ultrasonication for 15 min with the addition of 20 mL of isopropyl alcohol to wet the CNFs. The mixture was further vigorously stirred for 2 h. Finally, the products were collected by vacuum filtration and washed with deionized water, ethanol, and acetone several times. The free-standing CNF fabric thus formed is a flexible film after drying for 24 h at 50 °C in a vacuum oven, which can be easily peeled off the filter membrane. The CNF fabric was then punched out in circular disks with 1.2 cm diameter (1.13 cm^2), 1.9−2.0 mg mass, and ∼0.15 mm thick.

For the CNF/AC composite electrode synthesis, 48.0 mg of CNF powder and 48.0 mg of activated carbon powder were dispersed into 100 mL of 10 M HNO_3 solution. The mixture was pretreated for 18 h and washed with copious amount of deionized water. Then, the mixed CNF/AC powders were dispersed in 500 mL of deionized water by high-power ultrasonication for 15 min with the addition of approximately 20 mL of isopropyl alcohol. The mixture was further vigorously stirred for 2 h. Finally, the products were collected by vacuum filtration and washed with deionized water, ethanol, and acetone several times. After 24-h drying at 50 °C in a vacuum oven, the free-standing CNF/AC composite fabric was peeled off from the filter membrane and punched out into circular discs with 1.2 cm diameter (1.13 cm^2), 3.8−4.0 mg mass, and ∼0.20 mm thick.

2.4. Battery Assembly, Performance Test, and Electrochemical Experiments. The Li||LiSICON||polysulfide batteries were tested with a coin cell configuration (CR2032). The cells were assembled in an Ar-filled glovebox. First, appropriate amount of lithium polysulfide catholyte was added into the CNF or CNF/AC fabric electrode. The amount of catholyte used in the cell depends on the targeted sulfur loading of the cell and the concentration of the polysulfide used for the cell assembly. The sulfur content in the cathode matrix was maintained at 50−55%. Then, a piece of LiSICON membrane (with the thickness of ∼300 μm) was placed on top of the CNF or CNF/AC electrode. After that, a piece of polypropelene (PP) interlayer (with a thickness of 25 μm) which has been presoaked with the blank electrolyte (including the mixed solvent DME/DOL and the lithium salts $LiCF_3SO_3$ and $LiNO_3$, but without polysulfide) was attached onto the LiSICON membrane. Finally, the lithium metal foil anode was placed on the PP interlayer. Then, the coin cell was sealed inside the glovebox.

The charge/discharge performances of Li||LiSICON||polysulfide coin cells were evaluated between various cutoff voltages on a battery tester (Arbin instrument) at ambient temperature. The capacity values shown in this paper are calculated by dividing the capacities obtained by the mass of sulfur within the catholyte.

The ionic conductivity of the LiSICON membrane was determined with the conventional AC impedance method with two electrodes. The LiSICON (with a thickness of ∼350 μm) membrane was coated with gold before impedance measurement. The impedance was measured with a Solartron 1287 potentialstat, employing two blocking stainless steel electrodes. The frequency selected was from 1 MHz to 0.1 Hz. Electrochemical impedance spectra (EIS) measurements were conducted with a Solartron 1287 potentialstat. Frequency selected was from 1 MHz to 0.1 Hz.

2.5. Characterization. Morphological characterizations were carried out with either a Hitachi S-5500 (for CNF/AC electrode) or a FEI Quanta 600 (for CNF electrode) scanning electron microscope

DOI: 10.1021/acsami.5b04209
ACS Appl. Mater. Interfaces 2015, 7, 16625−16631

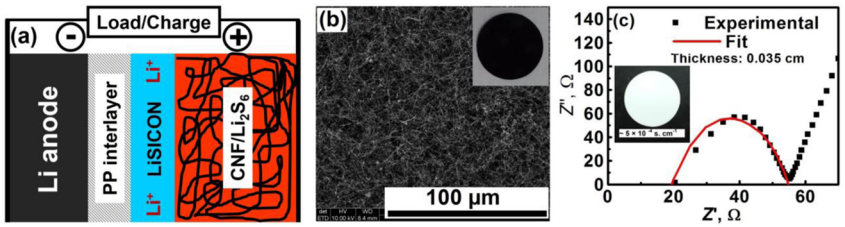

Figure 1. (a) Schematic of a hybrid lithium-dissolved polysulfide battery with a lithium super ionic conductor (LiSICON) membrane. (b) Scanning electron microscopy (SEM) image and a photograph (inset) of a carbon nanofiber (CNF) fabric electrode. (c) Electrochemical impedance spectroscopy (EIS) of a piece of LiSICON membrane in a symmetric electrochemical cell with two blocking stainless steel electrodes. Inset: Photograph of a piece of LiSICON membrane.

(SEM). The elemental distribution results were examined with an energy-dispersive spectrometer (EDS) attached to the Hitachi S-5500 and FEI Quanta 600 SEM. Surface profilometry of the LiSICON membrane was measured with a Veeco DEKTAK 150 profilometer.

3. RESULTS AND DISCUSSION

3.1. Concept of the Hybrid Li-PS Battery System and Retention of Polysulfides by the LiSICON Membrane. The battery configuration of a hybrid Li-PS cell is displayed in Figure 1a, in which the LiSICON-type solid Li-ion conductor serves both as an electrolyte and as a separator. A piece of polypropylene (PP) "soft" interlayer has to be placed between the solid separator and the Li anode to build a facile Li-ion migration path at the Li-metal/solid-electrolyte interface (will be further discussed in the next section) and to avoid the reduction of Ti^{4+} in contact with Li metal. A well-developed lithium polysulfide catholyte in our group[21−23] is used as the active cathode material, which comprises 1.5 or 4.0 M sulfur with a nominal molecular formula of Li_2S_6 in 1.0 M $LiCF_3SO_3$ and 0.1 M $LiNO_3$ in dimethoxy ethane (DME) and 1,3-dioxolane (DOL) (1:1 v/v). In this study, we preliminarily employ a simple-structure with a fabric electrode prepared with a low-cost carbon nanofiber material (as characterized with scanning electron microscope in Figure 1b, and pictured in the inset of Figure 1b) instead of using specialized composites or adopting any surface chemistry modification to demonstrate that the observed improvement in cyclability of the Li-PS cell is only contributed by the application of the nonporous ceramic solid electrolyte. Then, we employ a high-surface-area composite electrode for demonstration of the high-capacity-density Li-PS batteries (will be presented in section 3.5). The Li-ion solid-electrolyte membrane (as pictured in Figure 1c inset) developed by Ceramatec, Inc. has a Li-ion conductivity of $\sim 5 \times 10^{-4}$ S. cm^{-1} at room temperature (as measured with electrochemical impedance spectroscopy (EIS), Figure 1c), which is an acceptable value for the Li-based batteries under certain application conditions.

The use of the nonporous LiSICON solid electrolyte shows important advantages over the traditional porous separators in terms of suppressing polysulfide permeation. To optically determine the retention of polysulfide species by the solid LiSICON membrane, a setup schematized/pictured in Supporting Information Figure S1 is used. Thereby, a 4.0 mL solution of 0.25 M Li_2S_6 (nominal concentration) in DME/DOL (1:1, v/v) is placed inside a 10 mL transparent tube, whereas the opposite side of the membrane is filled with a pristine mixture of 40 mL of DME:DOL (1:1, v:v). During the experiment, the solutions rested without movement to exclude external influence on the diffusion test of polysulfides through the membrane. The resulting color change is evaluated by visual examination, as demonstrated in Supporting Information Figure S2a-e. As was predicted, the porous Celgard separator did not suppress the diffusion of polysulfides, thus the color of the DME/DOL solution is changed from colorless to light yellow after ~1 h of rest because of the diffusion of long chain polysulfides from the reservoir through the Celgard separator (Supporting Information Figure S2b). In contrast, the solid LiSICON membrane effectively suppressed the diffusion of polysulfide species. After 5 h of rest, no color change of the DME/DOL solvent was observed (Supporting Information Figure S2e).

3.2. Enhancement of Ionic Interface between the Li-Anode and the LiSICON Solid Electrolyte. Although the polysulfide migration is suppressed, the use of LiSICON solid electrolyte brings an unexpected problem with the Li-PS batteries, which generally exists in the low-temperature electrochemical reaction systems involving ceramic solid electrolytes. It has always been technically difficult to build a facile ionic-path at the metal/ceramic interface in an electrochemical system. Such an issue arises in the Li-PS cells with the LiSICON membrane as well, and the ionic interface between the Li anode and the LiSICON membrane plays an important role for the cell performance. Surface profilometric measurements of the LiSICON membrane are presented in Figure 2a

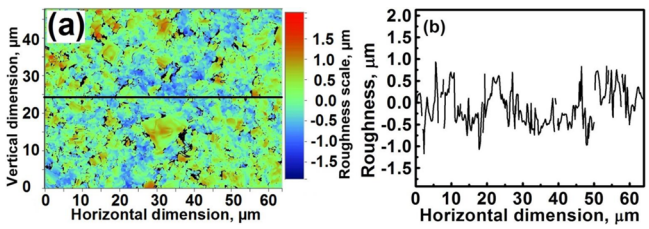

Figure 2. (a) Surface profilometry of the LiSICON membrane. (b) Roughness profile of the LiSiCON membrane along the horizontal line shown in (a).

and b, which show up to 1-μm (μm)-scale roughness of the membrane surface. Although lithium metal is relatively "soft" in comparison to the other common metallic materials, it is still difficult to maintain a perfect surface contact between Li-anode and the ceramic LiSICON membrane. Therefore, the ionic transfer path at the Li/LiSICON membrane interface is a serious challenge.

Initially, we tried two approaches to improve the ionic interface. One approach is to apply a layer of liquid blank electrolyte between the Li-anode and the LiSICON membrane (Figure 3a). Another approach is to apply a mechanical pressure to improve the mechanical contact between the LiSICON membrane and the Li metal (Figure 3b). However,

DOI: 10.1021/acsami.5b04209
ACS Appl. Mater. Interfaces 2015, 7, 16625−16631

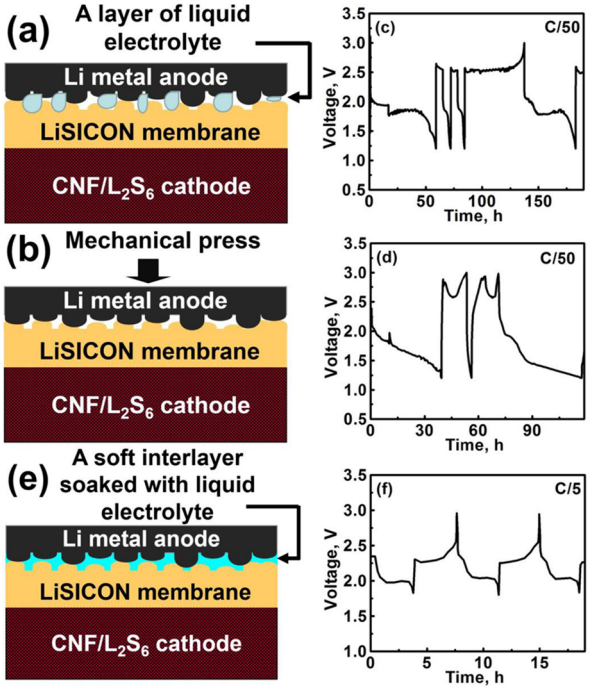

Figure 3. (a, b, and e) Schematic of the membrane-electrode assemblies (MEA) for the hybrid Li||LiSICON||polysulfide batteries (a) with the application of a layer of liquid electrolyte at the Li-anode/LiSICON membrane interface, (b) with the application of a mechanical pressure to enhance the surface contact between Li metal and the LiSICON membrane, and (e) with the insertion of a soft, facile Li-ion transfer interlayer to accommodate the roughness at the Li anode/LiSICON membrane interface. (c, d, and f) Voltage profiles of the Li||LiSICON||polysulfide batteries prepared with the MEAs shown in panels a, b, and e, respectively.

neither of these two methods can provide an effective way to improve the ionic interface. Figure 3c shows the voltage profile of the cell assembled with a layer of liquid blank electrolyte between the LiSICON and the Li-anode. The cell is operable at very low C-rates (<C/50), but exhibits an unsmooth voltage profile. At high rates of cycling, the cell shows fairly high polarization behavior and is not able to sustain the relatively high current applied to the cell. Figure 3d presents the voltage profile of the cell assembled with an attempt to improve the mechanical contact between the LiSICON and the Li metal. However, the cell is almost not able to sustain even the low cycling rate because of the high impedance at the Li/LiSICON membrane interface.

According to the characteristics at the Li-anode/ceramic solid electrolyte interface, we applied a layer of soft polymer material (polypropylene) in between the Li-metal and the LiSICON membrane to accommodate the roughness of the material surfaces. In addition, a blank liquid electrolyte consisting of 1.0 M $LiCF_3SO_3$ and 0.1 M $LiNO_3$ in DME/DOL mixture (1:1 v/v) was presoaked into the polypropylene separator (Figure 3e) to provide a facile medium for the Li-ion transfer. Performance of the cell is greatly improved by the insertion of such a liquid−electrolyte-integrated soft polymer interlayer (Figure 3f). The electrochemical impedance spectroscopy (EIS) data of the three types of membrane−electrode assemblies (MEAs) as illustrated in panels a, b, and e are provided in Supporting Information Figure S3, from which a significant improvement in the ionic conductivity of the MEA can be observed when a presoaked interlayer/separator is applied.

As we have presented in our previous studies, the active sulfur material Li_2S_6 in the catholyte is in a half charge/discharge state, which can be either first charged or discharged.[21−23] In this study, the cells were all first discharged for the cell performance studies. Figure 3f shows the voltage profile of the cell assembled with the approach presented in Figure 3e. During first discharge, a single-voltage plateau is seen, which depicts the process of the conversion of long-chain lithium polysulfide into short-chain lithium polysulfide or lithium disulfide. The subsequent charge/discharge curves show the characteristic, typical charge/discharge voltage profiles of the regular Li−S batteries (Supporting Information Figure S4). The smoothness of the voltage profile and the matched charge/discharge voltages to the transition processes of the regular sulfur cathode (comparison of charge/discharge voltages shown in Figure 3f and Supporting Information Figure S4) indicate that an excellent ionic interface has been developed with the approach shown in Figure 3e.

3.3. Electrochemical Performances and Cyclability Enhancement of the Hybrid Li-PS Batteries with the LiSICON Solid Electrolyte. Upon addressing the key ionic-conductivity issue at the Li/LiSICON interface, electrochemical performances of a series of Li||polypropylene/LiSICON||polysulfide cells were systematically evaluated with a coin-type configuration (as illustrated in Supporting Information Figure S5) at different cycling rates. Cell specifications and operation conditions of these cells are as listed in Supporting Information Table S1. Specially, for this set of experiments, 4.0 M sulfur catholytes (in the stoichiometric form of Li_2S_6) were used at the cathode. Figure 4a shows the representative charge/discharge profiles (at the third cycle) of the Li||LiSICON||polysulfide cells operated under various cycling rates of C/10, C/5, and C/3 (the detailed charge/discharge profiles of these cells at different cycles are presented in Supporting Information Figure S6). Similar to the regular Li−S batteries,[27,28] the voltage polarization of the cell becomes more and more prominent (voltage gap between charge and discharge profiles) with the increase in cycling rate. The cells exhibit initial discharge capacities (based on the sulfur active mass within the catholyte used) of ∼1200, ∼1100, and ∼1000 mAh g^{-1}, respectively, at C/10, C/5, and C/3 rates which correspond to ∼1.5, ∼1.3, and ∼1.2 electron transfer per sulfur atom.

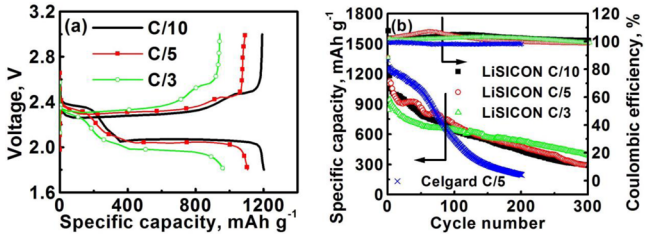

Figure 4. (a) Charge/discharge profiles of the hybrid Li||LiSICON||polysulfide batteries at various cycling rates. (b) Discharge capacities and Coulombic efficiencies of the hybrid Li||LiSICON||polysulfide batteries at different C-rates. Results of a Li-PS cell with a Celgard separator are provided for a comparison.

Figure 4b shows the discharge capacities and Coulombic efficiencies of the Li||LiSICON||polysulfide cells as a function of cycle number. Discharge performance of a Li-PS cell with a

DOI: 10.1021/acsami.5b04209
ACS Appl. Mater. Interfaces 2015, 7, 16625−16631

conventional Celgard membrane is presented here for a comparison. The cell with the Celgard membrane shows higher initial discharge capacities than the Li||LiSICON||polysulfide cells because of the fast ionic transportation in the liquid electrolyte integrated Celgard membrane. However, degradation in the discharge capacity of the cell with the Celgard separator becomes faster after ~60 cycles caused by the polysulfide shuttle behavior through the porous Celgard membrane. ~80 cycles later, the discharge capacities of the Li||LiSICON||polysulfide cells exceed that of the cell with the Celgard separator. Noticeably, the cells with the LiSICON membrane solid electrolyte show higher Coulombic efficiencies than that with the Celgard membrane, further evidencing the advantage of the LiSION membrane for the suppression of polysulfide shuttling.

3.4. Ionic Conductivity Maintenance of the LiSICON Membrane under the Electrochemical Cycling Conditions. The voltage profiles shown in Figure 4a and Supporting Information Figure S6 provide information about the voltage polarization of the Li||LiSICON||polysulfide cells during cycling at different rates. At lower C-rates, such as C/10, the charge/discharge voltage did not change too much with cycling. However, at relatively higher rates, such as C/5 and C/3, the voltage polarization increases relatively more significantly (Supporting Information Figure S6). To confirm the polarization-gain phenomenon of the cells at high C rates, the impedance of a Li||LiSICON||polysulfide cell was measured after cycling the cell at a C/3 rate for various times. The impedance variations during cycling are summarized in Supporting Information Figure S7a and b. As seen in Supporting Information Figure S7, both the bulk resistance (R_L) and the charge transfer impedance (R_{ct}) of the cell decrease slightly during the first few cycles and starts to increase after 20 cycles. Then, both of them became relatively stable after 40 cycles. However, the increase in either the voltage polarization or the cell impedance does not really mean the loss of the ionic conductivity of the LiSICON membrane. As a whole cell, the overall polarization in voltage profiles may be caused by many factors, such as the degradation of Li-anode, formation of solid-electrolyte interphase (SEI) at the cathode or at the anode, etc.[7,22] The above-mentioned effects are beyond the scope of this paper. Here, to verify the electrochemical compatibility of the LiSICON membrane with the polysulfide catholyte and avoid the intrinsic chemical reaction between the Li-anode and the polysulfides, a symmetric cell prepared with a nickel foam as the current collector was designed, as illustrated in Figure 5a. Two pieces of CNF paper was used at each side as a reservoir for the polysulfide catholyte. A piece of LiSICON membrane was placed in between. The polysulfide used in this cell comprises 4.0 M sulfur in the stoichemical form of Li_2S_6. The cell was cycled at a constant current of 2.0 mA cm^{-2}, a 3-h charge and 3-h discharge time frame, to simulate the real operating conditions of the Li||LiSICON||polysulfide cells (as illustrated in Figure 5b). The voltage profile of this symmetric cell provided in Figure 5c shows a few bumpy cycles (most likely due to the conditioning of the cell) at the beginning, and then the voltage profile becomes smooth after 5 cycles. The selected voltage profiles at different cycles are displayed in Figure 5d. It is obvious that the charge/discharge voltage gap does not increase with cycling of the cell, indicating that the impedance of the LiSICON membrane does not increase under the electrochemical cycling conditions.

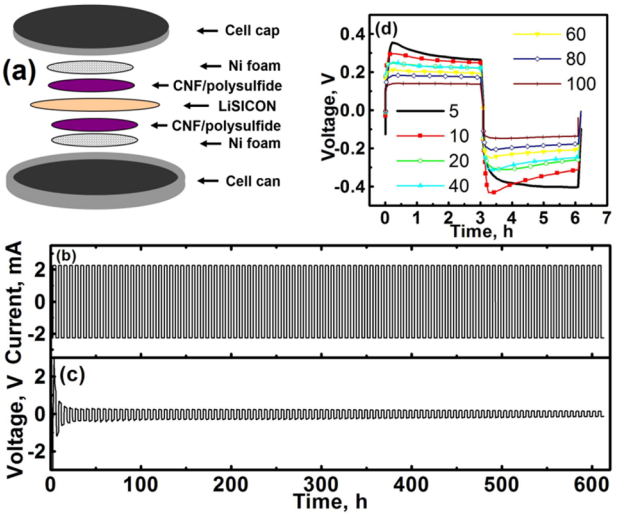

Figure 5. (a) Schematic of a symmetric Ni/polysulfide || LiSICON || polysulfide/Ni coin cell. (b) Square-wave current applied to the Ni/polysulfide||LiSICON||polysulfide/Ni coin cell. The cell was charged/discharged at a constant current density of 2.0 mA cm^{-2}. Charge/discharge durations are 3-h each. (c) Voltage profiles of the Ni/polysulfide||LiSICON||polysulfide/Ni symmetric coin cell. (d) Selected voltage profiles of the Ni/polysulfide||LiSICON||polysulfide/Ni symmetric coin cell at representative cycles.

The results of polysulfide permeation test shown in Supporting Information Figure S2 indicate that the LiSICON membrane exhibits significant advantages over the porous Celgard membrane for prevention of polysulfide shuttling. To further confirm this advantage under the electrochemical cycling conditions in the Li||LiSICON||polysulfide cells, ex-situ scanning transmission electron microscopy along with the energy dispersive X-ray spectroscopic (SEM/EDX) analyses were performed to a piece of LiSICON membrane after 20 cycles. Figure 6a and b show the cross-section image and the elemental distribution along the cross section. The x axis in Figure 6b starts from the LiSICON membrane facing to the cathode. The element titanium originated from the LiSICON membrane is displayed here as a reference. For a comparison,

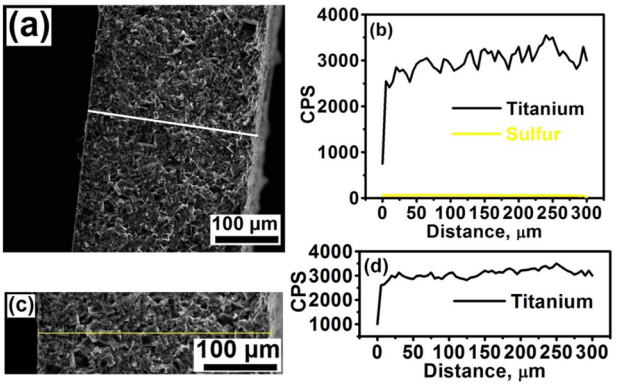

Figure 6. (a) Scanning electron microscopy (SEM) image of the cross-section of a cycled LiSICON membrane. (b) Elemental distribution of sulfur and titanium along the cross-section of the cycled LiSICON membrane, as indicated with the white line in (a). (c) SEM image of the cross-section of a pristine LiSICON membrane. (d) Elemental distribution of titanium along the cross-section of the pristine LiSICON membrane, as indicated with the white line in panel c.

DOI: 10.1021/acsami.5b04209
ACS Appl. Mater. Interfaces 2015, 7, 16625−16631

SEM/EDS analysis of an uncycled LiSICON membrane is provided in Figure 6c and d. The line-scan EDX (Figure 6b) profile does not show the obvious signal of elemental sulfur across the membrane, indicating that the polysulfide species does not penetrate through the LiSICON membrane during electrochemical cycling of the cell. There is a slight increase in the Ti content along the cross-section of the cycled LiSICON membrane, which may be originally from the LiSICON membrane, since the uncycled sample also showed a tendency of increase in the Ti content along the cross-section (Figure 6d).

So far, according to the results we obtained, the benefits of using the LiSICON membrane have been successfully demonstrated by the polysulfide diffusion experiments (Supporting Information Figure S2), the electrochemical cycling performance characterizations (Figure 4), and the SEM/EDS analysis of the cycled LiSICON membrane (Figure 6). Our ongoing and future work with the LiSICON membrane approach includes a series of applied research as well as a deep insight into the mechanistic investigations. Since the LiSICON membrane effectively suppresses the migration of the polysulfides from the cathode to the anode, the electrolyte additive $LiNO_3$ might not be necessary in Li−S cells, but it needs to be confirmed with future experiments.

Also as seen in Figure 4 and Supporting Information Figure S6, although the cycle life of the Li−S cells has been significantly improved by the LiSICON solid electrolyte approach, the discharge capacity of the hybrid Li−S cells still continuously decreases during electrochemical cycling. Actually, the decrease in the higher voltage plateau might be induced by a few factors. Even in the case that the polysulfide shuttle has been effectively suppressed, the anode degradation and the passivation of the active sulfur material in the cathode can also result in a loss of the discharge capacity. Therefore, development of effective methodologies for Li-anode protection and advanced cathode matrix materials are also two important aspects for our future research efforts.

3.5. High Capacity Li||LiSICON||Polysulfide Batteries. Upon verifying the advantages of the LiSICON membrane in eliminating polysulfide migration, high capacity Li||LiSICON||polysulfide cells with a high sulfur loading at the cathode were explored. In order to enhance the accommodation ability (accommodation of the charge/discharge products) of the cathode matrix, a composite electrode prepared with a high-surface-area activated carbon powder dispersed into interwoven carbon nanofiber fabric (CNF/AC) was developed. Activated carbon materials with high porosity can usually provide extremely high surface area for chemical or electrochemical reactions, but such powder materials are not able to form a robust electrode without nonactive binder materials. The low-cost carbon nanofiber materials possess self-weaving property, but have relatively lower surface area. The composite CNF/AC electrode developed here takes the combined advantages of the high-surface-area of activated carbon and the self-weaving property of CNF. Morphology of the composite CNF/AC electrode was characterized with STEM, as shown in Figure 7a. The interwoven CNF fabric has a single fiber diameter of ∼100 nm with micron-sized interspaces and ∼45 m^2 g^{-1} (the parameters are provided by Pyrograf Product, Inc.). The porous activated carbon filled in the interspaces of the CNF fabrics has a particle size of ∼50 nm (Figure 7a inset), surface area of 1500 m^2 g^{-1}, and pore volume of ∼2 mL g^{-1} (the parameters were provided by Sigma-Aldrich). The fine structure and high surface area of the composite CNF/AC fabric electrode provide facile properties for electrochemical reactions.

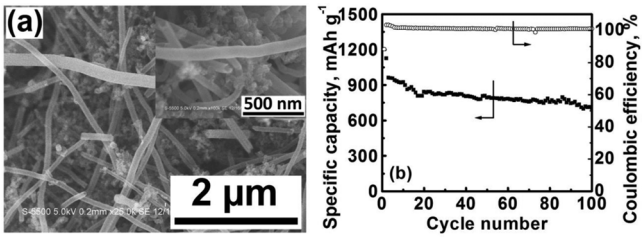

Figure 7. (a) Scanning electron microscopy (SEM) image of a carbon nanofiber/activated carbon composite electrode. (b) Discharge capacity and Coulombic efficiency of the hybrid Li||LiSICON||polysulfide battery with the CNF/AC composite cathode matrix and with 6.7 mAh g^{-1} cathode capacity.

Figure 7b shows the discharge capacity and Coulombic efficiency as a function of cycle number for a Li||LiSICON||polysulfide cell with a sulfur loading of 4.0 mg cm^{-2} (corresponding to a capacity density of 6.7 mAh g^{-1}) prepared with the CNF/AC composite cathode matrix. Compared to the cells with a capacity density of 2.85 mAh g^{-1} (Figure 4b), the higher capacity density leads to only a slightly lower reversible capacity (Figure 7). There is no significant difference in Coulombic efficiency between the cells compared in Figure 4b and Figure 7b. Moreover, the capacity degradation remains slow with high capacity density and the reversible capacity remains at >700 mAh g^{-1} after 100 cycles. The stable capacity delivery at high capacity density confirms that the Li||LiSICON||polysulfide cell is promising for practical high-energy-density battery applications.

4. CONCLUSIONS

A hybrid Li||LiSICON||polysulfide battery system has been developed by employing a LiSICON-type solid electrolyte as a cation-selective membrane. Use of the LiSICON membrane provides advantages over the porous Celgard separator for suppressing polysulfide diffusion. The lithium-polysulfide battery system with hybrid solid/liquid electrolytes exhibits significantly enhanced cyclability relative to the cells with the liquid electrolyte and porous Celgard separator. Ionic conductivity issue at the interface of lithium metal and the solid electrolyte can be addressed by an application of a "soft" polypropylene interlayer between the Li-anode and the LiSICON membrane. The solid LiSICON membrane maintains stable ionic conductivity under the electrochemical cycling conditions of the hybrid Li||LiSICON||polysulfide batteries. Coupling with a high-surface-area, high sulfur loading cathode, the hybrid Li||LiSICON||polysulfide cell delivers a remarkably stable capacity, promising for practical applications.

■ ASSOCIATED CONTENT

Supporting Information

Specifications and operating conditions for the hybrid Li-PS cells with the LiSICON membrane; schematic of a setup for polysulfide permeation experiments; polysulfide diffusion tests of the Celgard membrane and LiSICON membrane after various resting times; electrochemical impedance spectroscopy (EIS) data of the three types of membrane-electrode assemblies (MEAs); typical charge−discharge profiles of a Li−S cell prepared with a traditional sulfur−carbon cathode and a Celgard separator; schematic of the hybrid Li||LiSICON||po-

DOI: 10.1021/acsami.5b04209
ACS Appl. Mater. Interfaces 2015, 7, 16625−16631

lysulfide coin cell assembly; charge/discharge profiles of the hybrid Li||LiSICON||polysulfide batteries at different representative cycles at (a) C/10, (b) C/5, and (c) C/3 rates; EIS spectra and bulk resistance (R_L) as a function of cycle number of the Li−S cell with a LiSICON membrane solid electrolyte after various cycles at C/3 rate The Supporting Information is available free of charge on the ACS Publications website at DOI: 10.1021/acsami.5b04209.

AUTHOR INFORMATION

Corresponding Authors

*Tel: +1-801-433-3602. E-mail: fzhao@ceramatec.com.
*Tel: +1-512-471-1791. Fax: +1-512-471-7681. E-mail: manth@austin.utexas.edu.

Notes

The authors declare no competing financial interest.

ACKNOWLEDGMENTS

This work was funded in part by the Advanced Research Projects Agency-Energy (ARPA-E), U.S. Department of Energy, under Award Number DE-AR0000377.

REFERENCES

(1) Ibrahim, H.; Ilinca, A.; Perron, J. Energy Storage Systems - Characteristics and Comparisons. *Renewable Sustainable Energy Rev.* **2008**, *12*, 1221−1250.
(2) Chen, H. S.; Cong, T. N.; Yang, W.; Tan, C. Q.; Li, Y. L.; Ding, Y. L. Progress in Electrical Energy Storage System: A Critical Review. *Prog. Nat. Sci.* **2009**, *19*, 291−312.
(3) Yang, Z. G.; Zhang, J. L.; Kintner-Meyer, M. C. W.; Lu, X. C.; Choi, D. W.; Lemmon, J. P.; Liu, J. Electrochemical Energy Storage for Green Grid. *Chem. Rev.* **2011**, *111*, 3577−3613.
(4) Dunn, B.; Kamath, H.; Tarascon, J. M. Tarascon, Electrical Energy Storage for the Grid: A Battery of Choices. *Science* **2011**, *334*, 928−935.
(5) Goodenough, J. B.; Kim, Y. Challenges for Rechargeable Li Batteries. *Chem. Mater.* **2010**, *22*, 587−603.
(6) Manthiram, A.; Fu, Y. Z.; Su, Y. S. Challenges and Prospects of Lithium-Sulfur Batteries. *Acc. Chem. Res.* **2013**, *46*, 1125−1134.
(7) Manthiram, A.; Fu, Y. Z.; Chung, S. H.; Zu, C. X.; Su, Y. S. Rechargeable Lithium-Sulfur Batteries. *Chem. Rev.* **2014**, *114*, 11751−11787.
(8) Manthiram, A.; Chung, S.-H.; Zu, C. Lithium-sulfur Batteries: Progress and Prospective. *Adv. Mater.* **2015**, *27*, 1980−2006.
(9) Rauh, R. D.; Abraham, K. M.; Pearson, G. F.; Surprenant, J. K.; Brummer, S. B. Lithium-Dissolved Sulfur Battery with an Organic Electrolyte. *J. Electrochem. Soc.* **1979**, *126*, 523−527.
(10) Mikhaylik, Y. V.; Akridge, J. R. Polysulfide Shuttle Study in the Li/S Battery System. *J. Electrochem. Soc.* **2004**, *151*, A1969−A1976.
(11) Su, Y. S.; Manthiram, A. Lithium-Sulphur Batteries with a Microporous Carbon Paper as a Bifunctional Interlayer. *Nat. Commun.* **2012**, *3*, 1166.
(12) Ji, X. L.; Evers, S.; Black, R.; Nazar, L. F. Stabilizing Lithium-Sulphur Cathodes Using Polysulphide Reservoirs. *Nat. Commun.* **2011**, *2*, 325.
(13) Seh, Z. W.; Li, W. Y.; Cha, J. J.; Zheng, G. Y.; Yang, Y.; McDowell, M. T.; Hsu, P. C.; Cui, Y. Sulphur-TiO2 Yolk-Shell Nanoarchitecture with Internal Void Space for Long-Cycle Lithium-Sulphur Batteries. *Nat. Commun.* **2013**, *4*, 1331.
(14) Yang, Y.; Zheng, G. Y.; Cui, Y. Nanostructured Sulfur Cathodes. *Chem. Soc. Rev.* **2013**, *42*, 3018−3032.
(15) He, G.; Evers, S.; Liang, X.; Cuisinier, M.; Garsuch, A.; Nazar, L. F. Tailoring Porosity in Carbon Nanospheres for Lithium-Sulfur Battery Cathodes. *ACS Nano* **2013**, *7*, 10920−10930.
(16) Hassoun, J.; Scrosati, B. Moving to a Solid-State Configuration: A Valid Approach to Making Lithium-Sulfur Batteries Viable for Practical Applications. *Adv. Mater.* **2010**, *22*, 5198−5201.
(17) Hayashi, A.; Ohtomo, T.; Mizuno, F.; Tadanaga, K.; Tatsumisago, M. All-Solid-State Li/S Batteries with Highly Conductive Glass-Ceramic Electrolytes. *Electrochem. Commun.* **2003**, *5*, 701−705.
(18) Hayashi, A.; Ohtsubo, R.; Ohtomo, T.; Mizuno, F.; Tatsumisago, M. All-Solid-State Rechargeable Lithium Batteries with Li_2S as a Positive Electrode Material. *J. Power Sources* **2008**, *183*, 422−426.
(19) Kobayashi, T.; Imade, Y.; Shishihara, D.; Homma, K.; Nagao, M.; Watanabe, R.; Yokoi, T.; Yamada, A.; Kanno, R.; Tatsumi, T. All Solid-State Battery with Sulfur Electrode and Thio-LISICON Electrolyte. *J. Power Sources* **2008**, *182*, 621−625.
(20) Nagao, M.; Imade, Y.; Narisawa, H.; Kobayashi, T.; Watanabe, R.; Yokoi, T.; Tatsumi, T.; Kanno, R. All-Solid-State Li-Sulfur Batteries with Mesoporous Electrode and Thio-LISICON Solid Electrolyte. *J. Power Sources* **2013**, *222*, 237−242.
(21) Yu, X. W.; Manthiram, A. A Class of Polysulfide Catholytes for Lithium-Sulfur Batteries: Energy Density, Cyclability, and Voltage Enhancement. *Phys. Chem. Chem. Phys.* **2015**, *17*, 2127−2136.
(22) Fu, Y. Z.; Su, Y. S.; Manthiram, A. Highly Reversible Lithium/Dissolved Polysulfide Batteries with Carbon Nanotube Electrodes. *Angew. Chem., Int. Ed.* **2013**, *52*, 6930−6935.
(23) Zu, C. X.; Fu, Y. Z.; Manthiram, A. Highly Reversible Li/Dissolved Polysulfide Batteries with Binder-Free Carbon Nanofiber Electrodes. *J. Mater. Chem. A* **2013**, *1*, 10362−10367.
(24) Shin, B. R.; Nam, Y. J.; Kim, J. W.; Lee, Y. G.; Jung, Y. S. Interfacial Architecture for Extra Li^+ Storage in All-Solid-State Lithium Batteries. *Sci. Rep.* **2014**, *4*, 5572.
(25) Tatsumisago, M.; Nagao, M.; Hayashi, A. Recent Development of Sulfide Solid Electrolytes and Interfacial Modification for All-Solid-State Rechargeable Lithium Batteries. *J. Asian Ceram. Soc.* **2013**, *1*, 17−25.
(26) Wang, L.; Wang, Y.; Xia, Y. Towards High Performance Lithium-Ion Sulfur Battery Based on Li_2S Cathode Using Dual-Phase Electrolyte. *Energy Environ. Sci.* **2015**, *8*, 1551−1558.
(27) Kim, J. S.; Hwang, T. H.; Kim, B. G.; Min, J.; Choi, J. W. A Lithium-Sulfur Battery with a High Areal Energy Density. *Adv. Funct. Mater.* **2014**, *24*, 5359−5367.
(28) Oschatz, M.; Lee, J. T.; Kim, H.; Nickel, W.; Borchardt, L.; Cho, W. I.; Ziegler, C.; Kaskel, S.; Yushin, G. Micro- and Mesoporous Carbide-Derived Carbon Prepared by a Sacrificial Template Method in High Performance Lithium Sulfur Battery Cathodes. *J. Mater. Chem. A* **2014**, *2*, 17649−17654.

DOI: 10.1021/acsami.5b04209
ACS Appl. Mater. Interfaces 2015, 7, 16625−16631